OPEN ACCESS
International Journal of Bifurcation and Chaos, Vol. 30, No. 15 (2020) 2050258 (13 pages)

DOI: 10.1142/S0218127420502582

Multiple Hysteresis Jump Resonance in a Class of Forced Nonlinear Circuits and Systems

Maide Bucolo, Arturo Buscarino, Luigi Fortuna and Mattia Frasca
Dipartimento di Ingegneria Elettrica Elettronica e Informatica,
Università degli Studi di Catania,
viale A. Doria 6, 95125 Catania, Italy
CNR-IASI, Italian National Research Council – Institute for Systems Analysis and Computer Science "A. Ruberti", Rome, Italy

Received August 7, 2020

In this paper, a new class of systems with nonclassical jump resonance behavior is presented. Although jump resonance has been widely studied in the literature, this contribution refers to systems presenting a multiple hysteresis jump resonance phenomenon, meaning that the frequency response of the system presents more hysteresis windows nested within the same range of frequency. The analytical conditions for observing this type of behavior are derived and a design strategy to obtain multiple hysteresis jump resonance in circuits and systems presented.

Keywords: Nonlinear circuit; jump resonance; nonlinear dynamics; chaos.

1. Introduction

The nonlinear behavior of forced closed-loop systems can be marked by a frequency response with a jump resonance behavior. This phenomenon consists in the abrupt change in the amplitude of the system output when the frequency of the forcing signal is changed. Moreover, the jump in the amplitude does occur in different ways with respect to increasing or decreasing frequency. In principle, jump resonance can be viewed as a nonreversible behavior of forced nonlinear systems. The nonreversibility does include the presence of a trend showing hysteresis in frequency.

Jump resonance is well-known in forced nonlinear circuit and systems [Fukuma & Mutsubara, 1978; Lamba & Kavanagh, 1969]. It has been often considered as a undesirable behavior. Moreover, it has been successfully applied recently in frequency drift sensing and in applications referred to frequency monitoring devices [Buscarino *et al.*, 2020].

Jump resonance phenomena can be observed in systems and models typical of several scientific fields, ranging from civil [Yasui *et al.*, 1999] and mechanical [Murata *et al.*, 1987] engineering to fluids [Verhagen & Van Wijngaarden, 1965] and sound dynamics [Lee *et al.*, 2012]. Several attempts to model such phenomenon in real systems have been discussed [Padthe *et al.*, 2007; Tong & Lim, 2009] also keeping in view its use in the intentional design of jump resonance devices for sensing [Brenes *et al.*, 2016].

Methods to determine whether a system presents jump resonance are not universal. Moreover, compensators able to inhibit jump resonance cannot be assured. A wide literature does exist in the analysis of jump resonance phenomena, moreover, the positive role of systems with jump

resonance and the guidelines for their design have not been sufficiently studied.

In this paper, the positive effects of having jump resonance phenomena are considered. Previous approaches, exploiting the advantages of jump effects have been proposed in [Jabbari & Unruh, 2004; Salthouse & Sarpeshkar, 2006], and recent efforts in order to establish design conditions under which jump resonance is guaranteed have been recently addressed [Buscarino *et al.*, 2020; Buscarino *et al.*, 2018].

In the present study, closed-loop frequency responses where a unconventional jump resonance phenomenon occurs are considered. Multijump resonance is a new term that indicates frequency response with more hysteresis windows in different frequency ranges [Buscarino *et al.*, 2020]. This allows to have a frequency behavior that is selective as it includes different jumps occurring at diverse frequency windows, for decreasing and/or increasing frequencies. In this paper, we will instead focus on the case of multiple hysteresis behavior occurring within the same range of frequency.

Feedback systems with such characteristics will be proposed in this work. In particular, classical control schemes with a polynomial nonlinearity and a second order slightly damped linear system are considered. The conditions under which the system does work in the multiple hysteresis jump resonance mode have been obtained considering a fifth order static nonlinearity with only two terms, the cubic and the quintic.

The paper is organized as it follows. In Sec. 2, the jump resonance phenomenon is introduced and the main concepts of the multiple hysteresis jump resonance will be presented. Moreover, the adopted feedback scheme is reported. In Sec. 3, the analytical conditions under which the multiple hysteresis jump resonance exists are given, presenting detailed analytical and graphical tools. In Sec. 4, the main guidelines to design circuits and systems with specific frequency response characteristics will be given. In Sec. 5, experimental results are reported. Section 6, the generalization of the concept of multiple hysteresis jump resonance to higher order nonlinearities is outlined and the connection with a bifurcation route to chaos is explored. The conclusions will remark the main results obtained in the paper emphasizing the possibility of generalizing the strategy in order to match more complex closed-loop frequency responses to achieve systems with further selective frequency actions. Furthermore, a hint on the possible link between jump resonance and chaotic behavior in driven nonlinear systems is proposed.

2. From Jump Resonance to Multiple Hysteresis Jump Resonance Systems

Let us consider the closed-loop control scheme reported in Fig. 1, where

$$G(s) = \frac{K\omega_0^2}{s^2 + 2\xi\omega_0 s + \omega_0^2}, \tag{1}$$

and f is a cubic nonlinearity:

$$f(u) = u^3. \tag{2}$$

Let us consider now the describing function [Cook, 1994] of the previous nonlinearity:

$$N(U) = \frac{3U^2}{4}. \tag{3}$$

If the closed-loop equation of the system of Fig. 1 is considered, assuming

$$r(t) = \overline{R}\sin(\omega t - \psi), \tag{4}$$

and

$$u(t) = U\sin(\omega t), \tag{5}$$

it follows

$$\frac{3}{4}U^3 + G^{-1}(j\omega)U = \overline{R}e^{-j\psi}. \tag{6}$$

Let

$$R(\omega) = \Re[G^{-1}(j\omega)], \quad I(\omega) = \Im[G^{-1}(j\omega)], \tag{7}$$

from expression (6) it follows:

$$\frac{3}{4}U^3 + (R(\omega) + jI(\omega))U = \overline{R}\,e^{-j\psi}. \tag{8}$$

Taking the modulus of the complex number (8), it follows:

$$\left(\frac{3}{4}U^3 + RU\right)^2 + I^2U^2 = \overline{R}^2, \tag{9}$$

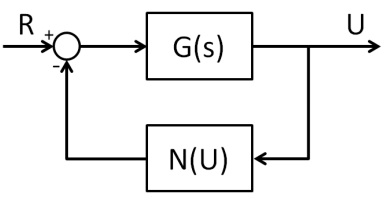

Fig. 1. Feedback scheme of the Lur'e representation.

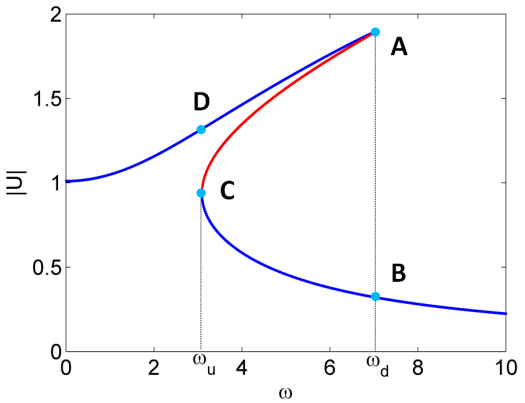

Fig. 2. Jump resonance behavior in the driven closed-loop nonlinear system in Fig. 1, with a cubic nonlinearity.

and therefore

$$\frac{9}{4}U^6 + \frac{3}{2}RU^4 + (R^2 + I^2)U^2 = \overline{R}^2. \qquad (10)$$

If it is assumed $U^2 = X$, the following cubic equation is obtained:

$$\frac{9}{4}X^3 + \frac{3}{2}RX^2 + (R^2 + I^2)X - \overline{R}^2 = 0. \qquad (11)$$

Assuming, for example $\xi = 0.5$, $K = 5$ and $\omega_0 = 1$, the frequency response for $\overline{R} = 1$ reported in Fig. 2 is obtained.

With reference to Fig. 2, for increasing values of the driving frequency the output will jump down at the frequency ω_d assuming a value U_d while if the frequency is decreasing the jump will occur at the frequency ω_u and the output will assume the values U_u. Indeed if the previous frequency response is analyzed, it is remarked that in the unstable frequency range between ω_u and ω_d, the cubic equation (11) admits three positive real solutions.

Between the points A and C there are three solutions. Two of them are multiple (two of the three collide in one respectively) at the points A and C, while in the other stable frequency ranges the cubic equation (11) admits only one real solution. In Fig. 2, it is therefore remarkable to note the frequency hysteretic behavior of the considered system.

The selectivity in the frequency of the system is also observed both with regards to the increasing or decreasing frequency trend of the input signal. Depending on the direction of the jump of U, it is possible to understand if the frequency is decreasing or increasing.

Let us consider the following case. The reference signal with constant amplitude has decreasing frequency so that the output amplitude jumps from C to D. When the frequency is increasing the amplitude goes to the point A and jumps to B. Therefore, we can detect only if the frequency drift followed a monotonic direction. In general, frequency drifts may follow more complex nonmonotonic paths, i.e. an increase occurring after a previous decrease and/or a following increase. These scenarios cannot be detected with the system in Fig. 1 with cubic nonlinearity.

Let us now consider the frequency response depicted in Fig. 3.

A constant amplitude reference signal with decreasing frequency is fed to the system, the output amplitude will jump from a to b when the frequency reaches ω_1. If now the frequency further decreases, the output amplitude will jump at the frequency ω_0 going from c to the state defined by the point d. If an increasing frequency signal is considered, at the frequency ω_2 we have the jump from point e to the point f. Let us consider again the decreasing frequency signal, the output state switches up at b, moreover, if the frequency at a following step increases, at ω_3 it switches from g to h. Therefore the state h represents the condition when the frequency at first decreases below ω_1 and then increases.

Assuming a circuit with a frequency response like that shown in Fig. 3, we achieve a state that overcomes the condition previously discussed referring to the frequency response of Fig. 2, thus improving the selective properties of the system. The state f defines an increasing frequency signal, the state b a frequency decreasing signal, the state d a further frequency decreasing signal, and the state h defines a frequency decreasing signal (until ω_1)

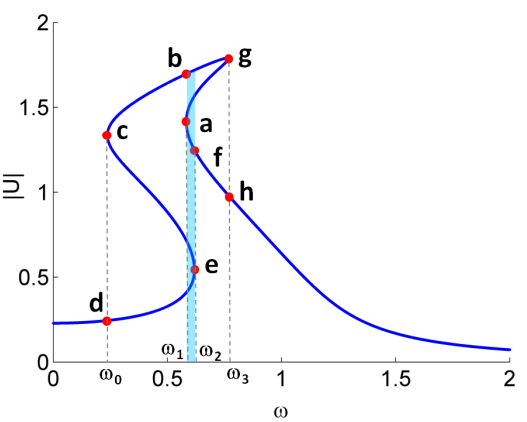

Fig. 3. Jump resonance behavior in the driven closed-loop nonlinear system in Fig. 1, with a quintic nonlinearity.

followed by an increasing frequency (up to ω_3). While the frequency ω_2 characterizes the jump up status in the frequency increasing behavior, the frequency ω_1 characterizes the jump up status in the frequency decreasing behavior.

Indeed a multiple hysteresis jump resonance system is established, characterized by the existence of the blue region in Fig. 3. In order to obtain a frequency response like that of Fig. 3, the strategy outlined in the following should be adopted.

The nonlinear frequency response shown in Fig. 3 is obtained by using a cubic nonlinearity that leads us to have the cubic expression (11). In [Buscarino *et al.*, 2020], it has been established under which conditions the system in Fig. 1 can have a frequency response like that shown in Fig. 2. The conditions are based on guaranteeing that the third-order equation admits three positive real solutions.

Now looking at Fig. 3, the conditions must ensure the existence of five positive real solutions in the hysteresis region, therefore a fifth-order (quintic) nonlinearity must be adopted. In fact in this case, the describing function corresponding to a quintic polynomial $f(u) = ax^5 + bx^3$ assumes the following form:

$$N(U) = AU^4 + BU^2, \tag{12}$$

and in accordance with the classical jump resonance approach the following equation is derived:

$$\begin{aligned} p_1(X) = X^5 &+ \left(\frac{2B}{A}\right) x^4 + \left(\frac{B^2 + 2AR}{A^2}\right) X^3 \\ &+ \left(\frac{2BR}{A^2}\right) X^2 + \left(\frac{I^2 + R^2}{A^2}\right) X - \frac{\overline{R}^2}{A^2} \\ &= 0, \end{aligned} \tag{13}$$

with $X = U^2$.

Equation (13) is a quintic equation in X. What are the conditions that allow to guarantee for the quintic the existence of the region, i.e. five positive real solutions? Even if a wide literature does exist for quintic polynomials [Barsan, 2009], conditions on the coefficients that guarantee the existence of five positive real solutions do not exist. In the following section, we will propose a strategy to determine some simplified conditions to get these results.

We add here a brief remark. Adopting a simplified quintic polynomial nonlinearity, i.e. $f(u) = ax^5$, leads to a describing function $N(U) = AU^4$. This implies that in the quintic equation (13), only odd power terms appear. In this case, a relationship among the five solutions of the polynomial is established [Barsan, 2009], and $x_1 + x_2 + x_3 + x_4 = -x_5$. The previous relationship is in contrast with searching for five positive real solutions, therefore a multiple hysteresis jump resonance cannot be observed by considering a nonlinearity $f(u) = ax^5$, and a further cubic term is fundamental.

3. Multiple Frequency Hysteresis: Analytical Conditions and Admissible Parameters Region

In order to guarantee the occurrence of a multiple hysteresis jump resonance, the quintic equation (13) must admit five real solutions. We assume that the limit condition at point a of Fig. 3 is searched. This implies that the ratio between the polynomial (13) and a second-order polynomial $p_2(x) = x^2 - 2a_L x + a_L^2$, must be with a remainder equal to zero. Therefore, it follows:

$$\frac{p_1(x)}{p_2(x)} = q(x) + \rho_1(x), \tag{14}$$

where the quotient is

$$q(x) = a_1 x^3 + b_1 x^2 + c_1 x + d_1, \tag{15}$$

with

$$\begin{aligned} a_1 &= 1, \\ b_1 &= 2a_L + \frac{2B}{A}, \\ c_1 &= 2a_L \left(2a_L + \frac{2B}{A} - a_L^2 + \frac{B^2 + 2AR}{A^2}\right), \\ d_1 &= \frac{2(B + 2Aa_L)(Aa_L^2 + Ba_L + R)}{A^2}. \end{aligned} \tag{16}$$

As concerns the remainder, it is:

$$\rho_1(x) = x f_1 + f_2, \tag{17}$$

with

$$\begin{aligned} f_1 = \frac{R^2}{A^2} &+ \left(\frac{6a_L^2}{A} + \frac{4Ba_L}{A^2}\right) R + 5a_L^4 \\ &+ 3\frac{B^2 a_L^2 + I^2}{A^2} + \frac{8Ba_L^3}{A}, \end{aligned} \tag{18}$$

and

$$f_2 = \frac{(\overline{R}^2 + 4A^2a_L^5 + 6ABa_L^4 + 4RAa_L^3 + 2B^2a_L^3 + 2RBa_L^2)}{A^2}. \tag{19}$$

In order for $r_1(x)$ to be zero, it must be $f_1 = 0$ and $f_2 = 0$.

Therefore, the following relationships hold

$$I^2 + R^2 + (6Aa_L^2 + 4Ba_L)R + 3B^2a_L^2 + 5A^2a_L^4 + 8ABa_L^3 = 0, \tag{20}$$

and

$$4A^2a_L^5 + 6ABa_L^4 + 4RAa_L^3 + 2B^2a_L^3 + 2RBa_L^2 = -\overline{R}^2. \tag{21}$$

In order to guarantee the multiple hysteresis jump resonance, the following conditions must be verified:

- Equation (20) must be satisfied;
- Equation (21) must be satisfied;
- The third-order polynomial $q(x)$ must have three real positive solutions.

In order to establish the last condition, a first constrain is given by the first column of the Routh table of the polynomial $q(x)$, since it must have terms with alternate signs. Building the Routh table we get

$$\begin{array}{lll} x^3: & a_1 & c_1 \\ x^2: & b_1 & d_1 \\ x^1: & C_1 & \\ x^0: & C_2 & \end{array} \tag{22}$$

where

$$C_1 = \left[\frac{B}{A}(B + Aa_L)\right] R + a_L^2 + \frac{3A^2BAL^2 + 4AB^2a_L + B^3}{A^2(B + Aa_L)} \tag{23}$$

and $C_2 = d_1$.

Then it must follow that

$$\begin{aligned} b_1 < 0 \;&\Rightarrow\; 2a_L + \frac{2B}{A} < 0 \Rightarrow B < -a_LA, \\ C_1 > 0 \;&\Rightarrow\; (23) > 0, \\ C_2 < 0 \;&\Rightarrow\; d_1 < 0. \end{aligned} \tag{24}$$

Moreover, the quantity

$$D = 18a_1b_1c_1d_1 - 4b_1^3d_1 + b_1^2c_1^2 - 4a_1c_1^3 - 27a_1^2d_1^2 \tag{25}$$

must be greater than zero [Barsan, 2009]. Taking into account relations (16),

$$D = -4(Aa_L^2 + Ba_L + r)F_1 = F_2F_1 \geq 0, \tag{26}$$

where

$$F_1 = \frac{50A^3a_L^4 + 70A^2Ba_L^3 + 60A^2Ra_L^2 + 17AB^2a_L^2 + 32ABRa_L + 8AR^2 - 3B^3a_L - B^2R}{A^4}. \tag{27}$$

Let us summarize the previous conditions establishing the regions where the quintic (13) admits five positive real solutions thus ensuring the multiple hysteresis jump resonance. In the map reported in Fig. 4, the regions where conditions (18), (19), (24) and (26) are satisfied, are shown. The map is drawn taking B on the x-axis and R on the y-axis, assuming A and a_L parameters greater than zero.

The admissible regions in the plane are first characterized by the relationships:

$$\begin{aligned} &B < -a_LA, \\ &F_2 \leq 0 \quad \texttt{and} \quad F_1 \leq 0, \\ &F_2 \geq 0 \quad \texttt{and} \quad F_1 \geq 0. \end{aligned} \tag{28}$$

Considering that Eq. (20) is quadratic in R, the admissible range is given by the condition on the discriminant $\Delta > 0$ that leads to the values of $B > -2a_LA$ and $B < -10a_LA$.

Taking into account the other conditions, the two admissible regions are those indicated by (1) and (2) in Fig. 4.

Moreover, in those regions $C_1 > 0$. The multiple hysteresis jump resonance region is characterized for $B > -2a_LA$ by the points external to $F_1 = 0$ (in blue in Fig. 4), while for $B < -10a_LA$ by its internal points. Moreover, for those points from (20), we get

$$I^2 = -R^2 + (6Aa_L^2 + 4Ba_L)R + 3B^2a_L^2 + 5A^2a_L^4 + 8ABa_L^3 > 0, \tag{29}$$

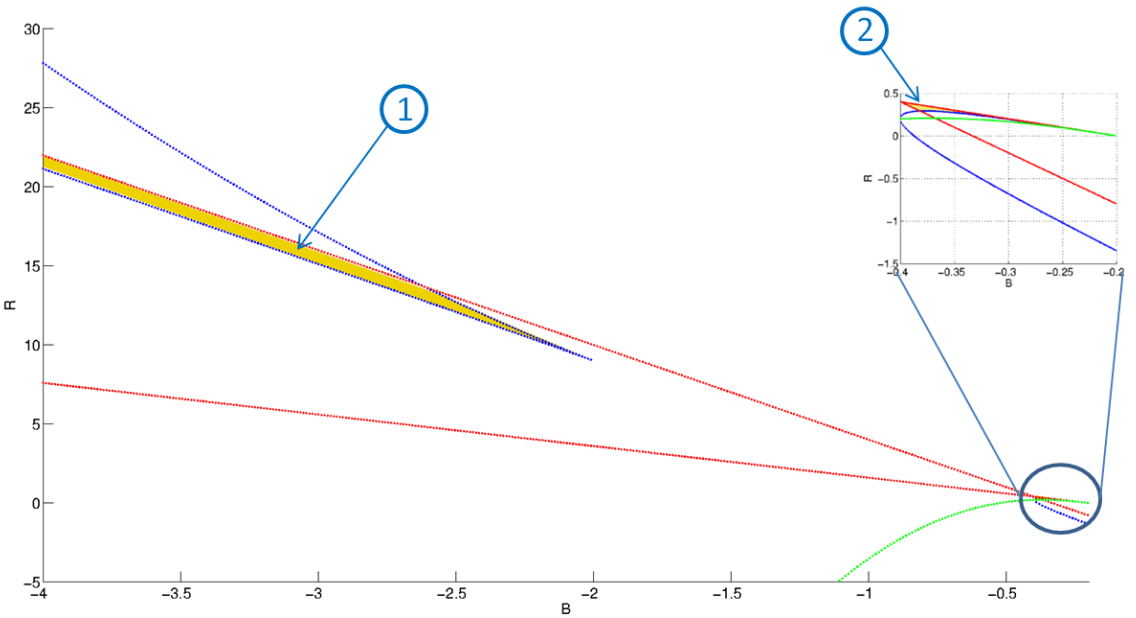

Fig. 4. Regions in the B–R parameter space satisfying conditions for multiple hysteresis jump resonance to occur: $F_1 = 0$ is reported blue, $F_2 = 0$ in red and $D = 0$ in green.

therefore the multiple frequency hysteresis points (B, R) are those contained respectively in the regions defined before.

In Fig. 5, the conditions are evaluated for $-20a_L A < B < -10a_L A$ with $A = 0.1$ and $a_L = 2$. The suitable region is colored in yellow.

Let us consider now the range $-2a_L A < B < -a_L A$ with $A = 0.1$ and $a_L = 2$, obtaining the region reported in yellow in Fig. 6.

For each value of B and R in the previously defined regions, Eq. (23) is congruent in the sense that we get

$$\overline{R}^2 = -2a_L^2(B + 2Aa_L)(Aa_L^2 + Ba_L + R). \quad (30)$$

Therefore, if we will take a closer look at the suitable region for $-2a_L A < B < -a_L A$, it corresponds to pairs of suitable B_i and R_i that allow us to have multiple hysteresis jump resonance, as reported in Fig. 7.

For I and R each segment s_i defines a suitable arc of the circles family (20), therefore from a graphical point of view after having chosen A, a_L and B, we can plot a circle, as that reported in Fig. 8.

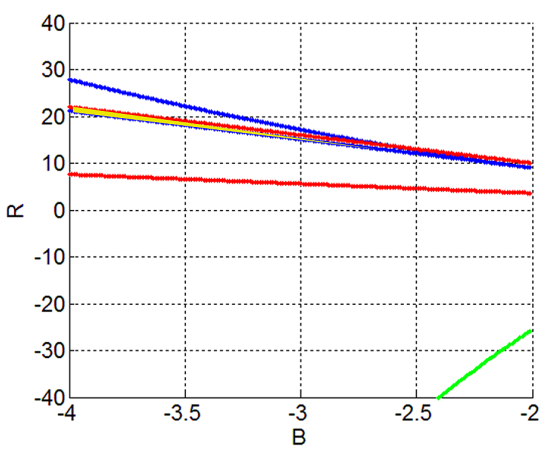

Fig. 5. Regions in the B–R parameter space satisfying conditions for multiple hysteresis jump resonance to occur evaluated for $-20a_L A < B < -10a_L A$ with $A = 0.1$ and $a_L = 2$: $F_1 = 0$ is reported blue, $F_2 = 0$ in red and $D = 0$ in green.

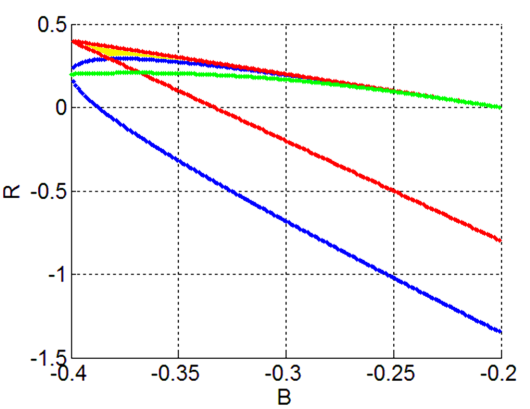

Fig. 6. Regions in the B–R parameter space satisfying conditions for multiple hysteresis jump resonance to occur evaluated for $-2a_L A < B < -a_L A$ with $A = 0.1$ and $a_L = 2$: $F_1 = 0$ is reported blue, $F_2 = 0$ in red and $D = 0$ in green.

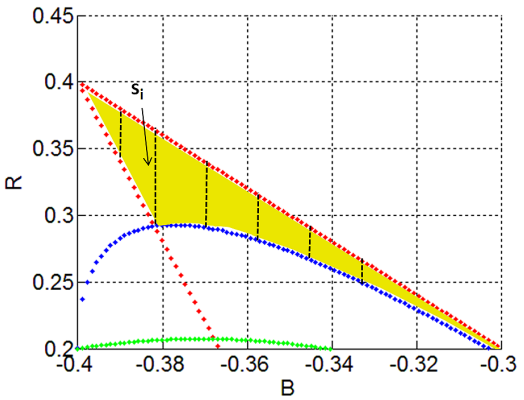

Fig. 7. Zoom on the admissible region in the B–R parameter space for $-2a_LA < B < -a_LA$ with $A = 0.1$ and $a_L = 2$: $F_1 = 0$ is reported blue, $F_2 = 0$ in red and $D = 0$ in green.

The Nyquist plot of $G^{-1}(j\omega) = R(\omega) + jI(\omega)$ is required to intersect the circle on the arc corresponding to a given s_i, in a particular point $P(R_i, I_i)$. Of course, given R_i, I_i, a_L, B, A, a value of $\overline{R}$ is computed by using the expression (23).

In Fig. 9 various plots of the function F_1 in the range $-2a_LA < B < -a_LA$ for different values of a_L are reported.

If we select $a_L = 2$ for $A = 0.1$ in the plot Fig. 6, for the value $B = -0.378$ and choosing $R_i = 0.3$, a value of $I_i = 0.02$ is obtained from (20). Assuming $G^{-1}(j\omega) = R(\omega) + jI(\omega)$ with $R(\omega) = \frac{-\omega^2+\omega_0^2}{K\omega_0^2}$ and $I(\omega) = \frac{2\xi\omega}{K\omega_0^2}$ for $\omega_0 = 1$, the equations $\frac{-\omega^2+1}{K} = 0.3$ and $\frac{2\xi\omega}{K} = 0.02$ give us $K = 2.202$ and $\xi = 0.08$. The value of $\overline{R} = 0.0995$ is given by Eq. (29).

In Fig. 10, the corresponding frequency response displaying multiple hysteresis jump resonance has been reported.

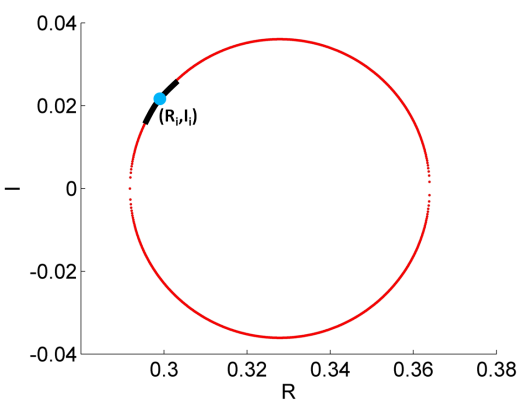

Fig. 8. Circle of the family (20) with $A = 0.1$ and $a_L = 2$, the arc corresponds to s_i with $B = -0.378$.

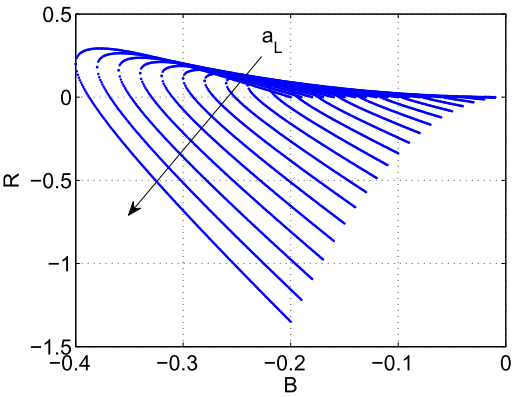

Fig. 9. F_1 in the range $-2a_LA < B < -a_LA$ for different values of $0.1 < a_L < 2$.

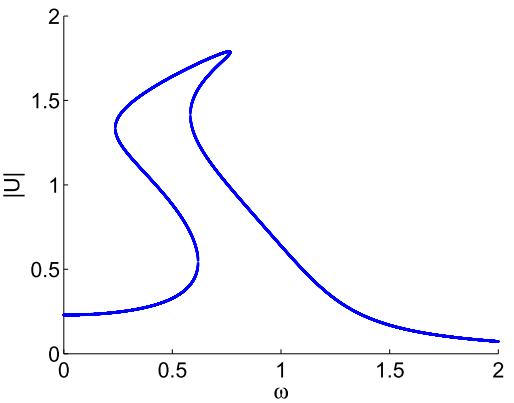

Fig. 10. Multiple hysteresis jump resonance for the system in Fig. 1 with quintic polynomial nonlinearity $f(u) = au^5 + bu^3$, with $A = 0.1$, $B = -0.378$ (corresponding to $a = 0.16$ and $b = -0.504$). The parameters of the linear part are chosen as $\omega_0 = 1$, $\xi = 0.08$ and $K = 2.202$.

4. Design of Multiple Hysteresis Jump Resonance Circuits and Systems: Guidelines

In the previous section, the analytical conditions in order to guarantee multiple hysteresis jump resonance systems have been discussed. In this section, the guideline to design circuits with multiple hysteresis jump resonance with assigned specifications in the frequency response is outlined. For $G(s)$, the following transfer function is assumed:

$$G(s) = \frac{K\omega_0^2}{s^2 + 2\xi\omega_0 s + \omega_0^2}. \tag{31}$$

If we consider $G^{-1}(j\omega) = R(\omega) + jI(\omega)$, then $R = \frac{\omega_0^2-\omega^2}{K\omega_0^2}$ and $I = \frac{2\xi\omega}{K\omega_0^2}$. The assigned parameters for designing the circuit are the quantities ω_1 (jump up) and ω_2 (jump down), the quantity a_L is fixed

so that the jump quantity is greater than a_L. In the following, we will choose $\omega_1 = 0.58$ and $\omega_2 = 0.62$.

Moreover the following relationships hold, $R_1 = \frac{\omega_0^2-\omega_1^2}{K\omega_0^2}$ and $R_2 = \frac{\omega_0^2-\omega_2^2}{K\omega_2^2}$, and $I_1 = \frac{2\xi\omega_1}{K\omega_0^2}$ and $I_2 = \frac{2\xi\omega_2}{K\omega_0^2}$. Therefore, it follows that $\frac{R_2}{R_1} = \frac{\omega_0^2-\omega_1^2}{\omega_0^2-\omega_2^2} = r_1$ and $\frac{I_2}{I_1} = \frac{\omega_2}{\omega_1} = r_2$.

If the frequency ω_0 is fixed, the project design requires that $\overline{R}$, ξ and K satisfy the previous specifications.

Example. Fixing $\omega_0 = 1$ and $a_L = 2$, Eq. (21) becomes

$$128A^2 + 96AB + 32RA + 16B^2 + 8RB = -\overline{R}^2. \tag{32}$$

Therefore, the equation that allows to obtain R_2 is

$$-4A^2a_{L_2}^5 - 6ABa_{L_2}^4 - 4Rr_1Aa_{L_2}^3 - 2B^2a_{L_2}^3 - 2Rr1Ba_{L_2}^2, \tag{33}$$

where a_{L_2} is the multiple solution at ω_2 (i.e. point e in Fig. 3). Moreover, Eq. (20) for $a_L = 2$ is solved with respect to I_1 and taking into account r_1 and R_1 we have the following equation:

$$I_1^2 + R_1^2 + (24A + 8B)R_1 + 12B^2 + 80A^2 + 64AB = 0. \tag{34}$$

Both equations must be satisfied and therefore the graphical solution reported in Fig. 11 can be obtained. We assumed $A = 0.1$ and $B = -0.378$ and we obtained $a_{L_2} = 0.3$ and $R_2 = 0.2989$. Therefore, $R_1 = 0.3$, $I_1 = 0.02$ and $I_2 = 0.04$.

So, we get $K = \frac{\omega_0^2-\omega^2}{\omega_0^2 R_1}$ and $\xi = \frac{KI_1}{2\omega_1}$. The value of $\overline{R}$ is derived by using the relation (23), the same value of course is obtained if $a_L = 2$ and $R = R_1$ or $a_L = a_{L_2}$ and $R = R_2$. We get $\overline{R} = 0.0995$.

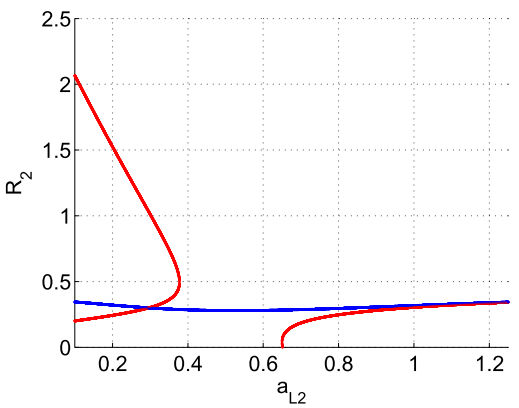

Fig. 11. Graphical solution of Eqs. (33) and (34).

5. Experimental Results

The multiple hysteresis jump resonance system designed in the previous sections has been implemented as a nonlinear electronic circuit based on off-the-shelf discrete components. The circuit encompasses only capacitors, resistors, standard operational amplifiers, we used $TL084$, and three cascading analog multipliers $AD633$ in order to realize the quintic polynomial nonlinearity. Different strategies can be adopted to realize the nonlinearity, such as circuits based on diodes [Buscarino *et al.*, 2017] obtaining a low-cost solution despite a lower accuracy in certain frequency ranges. In order to obtain a circuit which could be easily rescaled in frequency, we relied on the more robust approach based on analog multipliers. The schematic of the circuit showing multiple hysteresis jump resonance, the dynamical equations and the component values are discussed and reported in the Appendix. The frequency range of the multiple hysteresis jump resonance has been chosen so that $\omega_1 \approx 500$ rad/s and $\omega_2 \approx 660$ rad/s, which in terms of frequency correspond to $f_1 = 80$ Hz and $f_2 = 105$ Hz.

The circuit has been driven by a sinusoidal signal with peak-to-peak amplitude of 2 V and null offset, obtained by using an Agilent $33250A$ function generator. The frequency of the input signal is at first swept up between 10 Hz and 210 Hz, so that, referring to Fig. 3, the amplitude of the output signal would follow the path to point e jumping up to point f. In the second time, the frequency is swept down from 210 Hz and 10 Hz, thus reproducing the path jumping up to point a to point b, and then jumping down from point c to point d. The frequency responses of the circuit for the two cases have been measured by a Keysight $35670A$ Dynamic Signal Analyzer, averaging over 200 realizations. The experimental frequency responses are reported in Fig. 12, where the critical points are marked in according to Fig. 3.

In order to experimentally observe further the hysteresis window nested inside the multiple jump resonance range, i.e. path from a to b decreasing the frequency and then from g to h successively increasing the frequency, we used a sinusoidal signal sweeping from 100 Hz down to 70 Hz followed by a signal sweeping from 70 Hz to 100 Hz. The frequency responses evaluated by using the signal analyzer

Fig. 12. Experimental evaluation of the frequency response of the designed multiple hysteresis jump resonance circuit obtained by driving the system with a sinusoidal signal and peak-to-peak amplitude of 2 V and null offset. The two traces are related to frequency sweeping up (down) between 10 Hz and 210 Hz. Critical points are marked in accordance with Fig. 3.

averaging over 200 realizations are reported in Fig. 13, where again the critical points are marked according to Fig. 3.

The experimental results, thus, confirm the existence of multiple hysteresis jump resonance in the realized circuit. Moreover, the frequency range can be suitably rescaled by simply varying the capacitors used in the circuit, maintaining the structure of the schematic.

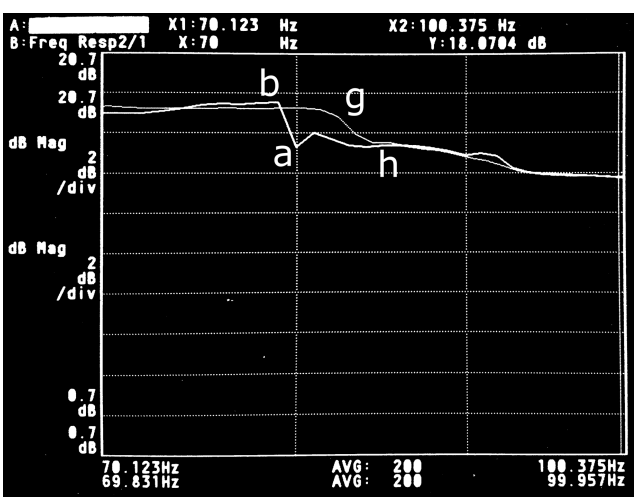

Fig. 13. Experimental evaluation of the frequency response of the designed multiple hysteresis jump resonance circuit obtained by driving the system with a sinusoidal signal and peak-to-peak amplitude of 2 V and null offset. The two traces are related to frequency sweeping down (up) between 70 Hz and 100 Hz. Critical points are marked according to Fig. 3.

6. Higher Order Multiple Hysteresis Jump Resonance and the Route to Chaos

The paper discusses the quintic nonlinearity and quintic frequency response. Moreover, the concept of multiple hysteresis jump resonance appears in a wider class of systems, where more hysteresis windows can be obtained within the same frequency range. The technique outlined in this paper can be extended to higher order polynomial nonlinearity, such as septic or nonic nonlinearities, which lead to more complex nested hysteresis windows. In the case of septic nonlinearity, seven positive real values for the frequency response at a given frequency can be retrieved, nine in the case of nonic nonlinearity, and so on. Clearly, deriving a closed form solution to these problems involves higher order geometrical considerations. Examples of septic and nonic nonlinearity leading to multiple hysteresis jump resonance are reported in Figs. 14 and 15. The existence of a range of frequency in which multiple values of the frequency response are retrieved is clearly shown.

A further interesting aspect linked to jump resonance and, more in general, with multiple hysteresis jump resonance is the fact that it can be conjectured that such phenomenon is a prelude for chaos. In fact, increasing the amplitude of the input signal, windows of chaotic behavior can be observed within the frequency range where jump resonance occurs. Moreover, higher order nonlinearities lead to a smaller scaling of the amplitude for the input signal to retrieve a chaotic attractor starting from the

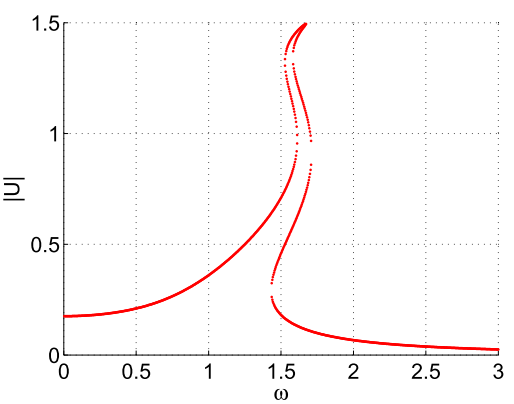

Fig. 14. Multiple hysteresis jump resonance in a closed-loop system as in Fig. 1 with septic nonlinearity of the form $f(u) = au^7 + bu^5 + cu^3$. The frequency response has been calculated for $K = 1$, $\xi = 0.04$, $\omega_0 = 1$, $a = \frac{7}{8}$, $b = -\frac{10}{3}$, $c = \frac{14.25}{4}$. The input signal is $r(t) = \overline{R}\sin(\omega t)$ with $\overline{R} = 0.2$.

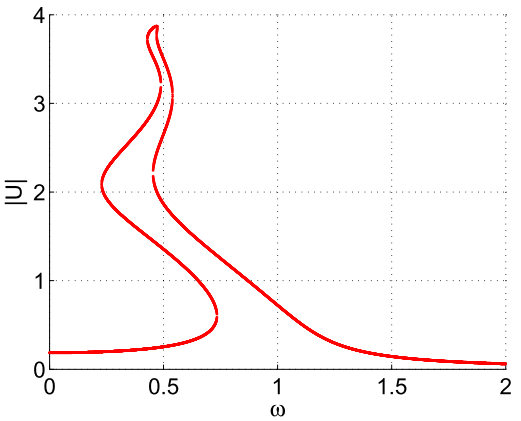

Fig. 15. Multiple hysteresis jump resonance in a closed-loop system as in Fig. 1 with nonic nonlinearity of the form $f(u) = au^9 + bu^7 + cu^5 + du^3$. The frequency response has been calculated for $K = 0.00019$, $\xi = 0.05$, $\omega_0 = 1$, $a = 1$, $b = -38.09$, $c = 499.68$, $d = -2569$. The input signal is $r(t) = \overline{R}\sin(\omega t)$ with $\overline{R} = 948$.

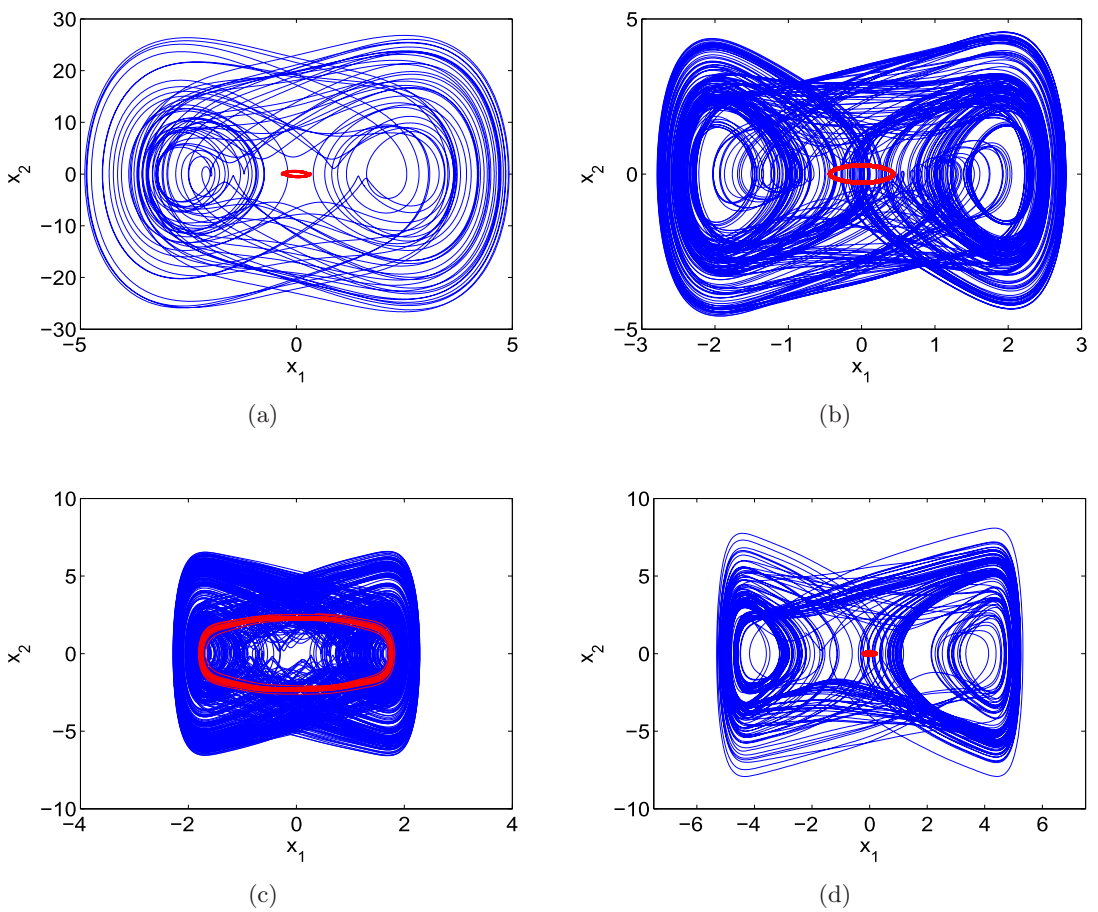

Fig. 16. Chaotic attractors (in blue) obtained from the system in Fig. 1 with (a) cubic $f(u) = ax^3$, (b) quintic $f(u) = ax^5 + bx^3$, (c) septic $f(u) = ax^7 + bx^5 + cx^3$ and (d) nonic $f(u) = ax^9 + bx^7 + cx^5 + dx^3$ polynomial nonlinearities. Parameters are: (a) $K = 5$, $\xi = 0.01$, $\omega_0 = 1$, $a = 0.75$, $\overline{R} = 15$ and $\omega = 3.4$ (blue), $\overline{R} = 0.2$ and $\omega = 3.4$ (red); (b) $K = 2.202$, $\xi = 0.08$, $\omega_0 = 1$, $a = 0.16$, $b = -0.504$, $\overline{R} = 5$ and $\omega = 0.6$ (blue), $\overline{R} = 0.0995$ and $\omega = 0.6$ (red); (c) $K = 1$, $\xi = 0.04$, $\omega_0 = 1$, $a = 0.875$, $b = -3.333$, $c = 3.5625$, $\overline{R} = 8$ and $\omega = 1.59$ (blue), $\overline{R} = 0.2$ and $\omega = 1.59$ (red); (d) $K = 0.00019$, $\xi = 0.05$, $\omega_0 = 1$, $a = 1$, $b = -38.09$, $c = 499.68$, $d = -2569$, $\overline{R} = 28740$ and $\omega = 0.49$ (blue), $\overline{R} = 958$ and $\omega = 0.49$ (red).

amplitude for which the multiple hysteresis jump resonance response has been calculated.

Let us consider the attractors in Fig. 16. They have been retrieved for the system in Fig. 1 with different order polynomial nonlinearities, ranging from cubic to nonic. Parameters of the nonlinearity as well as those of the linear part are reported in the figure caption. The amplitude and the frequency of the forcing signal $r(t) = \overline{R}\sin(\omega t)$ are appropriately chosen: in particular, the frequency is selected within the range of multiple solutions for the frequency response. In the same figure, we also report the periodic orbit obtained for the amplitude for which the frequency response has been calculated.

7. Conclusions

The new concept of multiple hysteresis jump resonance for a class of forced nonlinear circuits and systems has been presented, providing a complete analysis of the observed hysteretic behavior. The discussion on the role of these systems have been emphasized and studied in detail presenting an analytical strategy to obtain a complete understanding of such behavior and for a parametric study.

The analytical approach adopted introduces a general procedure to design circuits and systems with specific multiple hysteresis jump resonance in a desired frequency range. Even if the results are referred to second order systems, the main technique is quite general.

The mathematical limits of the polynomial algebra have been overcome with graphical techniques. Moreover, the numerical results, in spite of the classical criticality for polynomial techniques, are robust. In fact, working with symbolic expressions, the relationships are obtained in closed form.

The experimental results validate the behavior of nonlinear frequency response of the system. The suitability of both the design technique and the experimental implementation of the circuit has been discussed by using accurate measurements.

Moreover, we generalized the concept of multiple hysteresis jump resonance to higher order nonlinearities retrieving more nested hysteresis. Finally, we highlighted the connection between jump resonance and the onset of chaos in forced nonlinear systems. We can conjecture that increasing the order of the polynomial nonlinearity leads to more favourable conditions to obtain chaos, in the sense that a smaller scaling of the amplitude of the external inputs is needed to observe a bifurcation to chaos. This may be a further hint to understand the onset of complex dynamics in forced nonlinear circuits and systems.

References

Barsan, V. [2009] "Physical applications of a new method of solving the quintic equation," arXiv preprint arXiv:0910.2957.

Brenes, A., Juillard, J., Bourgois, L. & Dos Santos, F. V. [2016] "Influence of the driving waveform on the open-loop frequency response of MEMS resonators with nonlinear actuation schemes," *J. Microelectromech. Syst.* **25**, 812–820.

Buscarino, A., Fortuna, L., Frasca, M. & Sciuto, G. [2014] *A Concise Guide to Chaotic Electronic Circuits* (Springer International Publishing).

Buscarino, A., Fortuna, L. & Frasca, M. [2017] *Essentials of Nonlinear Circuit Dynamics with MATLAB and Laboratory Experiments* (CRC Press).

Buscarino, A., Caponetto, R., Famoso, C. & Fortuna, L. [2018] "Jump resonance in fractional order circuits," *Int. J. Bifurcation and Chaos* **28**, 1850016-1–9.

Buscarino, A., Famoso, C., Fortuna, L. & Frasca, M. [2020] "Multi-jump resonance systems," *Int. J. Contr.* **93**, 282–292.

Cook, P. A. [1994] *Nonlinear Dynamical Systems* (Prentice-Hall, Englewood Cliffs, NJ, USA).

Fukuma, A. & Matsubara, M. [1978] "Jump resonance in nonlinear feedback systems — Part I: Approximate analysis by the describing-function methods," *IEEE Trans. Autom. Contr.* **23**, 891–896.

Jabbari, A. & Unruh, A. [2004] "Jump resonance in audio transducers," *Audio Engineering Society Convention 117* (Audio Engineering Society).

Lamba, S. S. & Kavanagh, R. J. [1969] "Jump-resonance criteria for systems containing double-valued and frequency-dependent nonlinearities," *Proc. Instit. Electrical Engineers* **116**, 1225–1228 (IET Digital Library).

Lee, Y. Y., Li, Q. S., Leung, A. Y. T. & Su, R. K. L. [2012] "The jump phenomenon effect on the sound absorption of a nonlinear panel absorber and sound transmission loss of a nonlinear panel backed by a cavity," *Nonlin. Dyn.* **69**, 99–116.

Murata, A., Kume, Y. & Hashimoto, F. [1987] "Application of catastrophe theory to forced vibration of a diaphragm air spring," *J. Sound Vibr.* **112**, 31–44.

Padthe, A. K. & Bernstein, D. S. [2007] "A delay-Duhem model for jump-resonance hysteresis," *2007 46th IEEE Conf. Decision and Control* (IEEE), pp. 1609–1614.

Salthouse, C. D. & Sarpeshkar, R. [2006] "Jump resonance: A feedback viewpoint and adaptive circuit solution for low-power active analog filters," *IEEE*

Trans. Circuits and Systems I: *Reg. Papers* **53**, 1712–1725.

Tong, H. & Lim, K. S. [2009] "Threshold autoregression, limit cycles and cyclical data," *Exploration of a Nonlinear World: An Appreciation of Howell Tong's Contributions to Statistics* (World Scientific, Singapore), pp. 9–56.

Verhagen, J. H. G. & Van Wijngaarden, L. [1965] "Nonlinear oscillations of fluid in a container," *J. Fluid Mech.* **22**, 737–751.

Yasui, H., Marukawa, H., Momomura, Y. & Ohkuma, T. [1999] "Analytical study on wind-induced vibration of power transmission towers," *J. Wind Engin. Industr. Aerodyn.* **83**, 431–441.

Appendix A

The experimental setup is implemented following a state-variable approach [Buscarino *et al.*, 2014], which also allows to easily introduce a temporal scaling so that the multiple hysteresis jump resonance can be observed in the range of hundreds of Hz. This can be done by properly choosing capacitor values. This means that each block, including the nonlinearity, has to be rewritten as a system of nonlinear dynamical equations as:

$$\begin{aligned} \dot{x} &= y, \\ \dot{y} &= -2\xi\omega_0 y - \omega_0^2 x \\ &\quad + K\omega_0^2(-bx^3 - ax^5 + r(t)), \end{aligned} \tag{A.1}$$

where x and y are the two state variables of the second order system described by $G(s)$ as in Eq. (1), a and b are the nonlinearity coefficients, and $r(t)$ is the input signal. The implementation is based on the schematic reported in Fig. 17, where each capacitor is associated with a state variable of Eqs. (A.1). The circuit reported in Fig. 17 obeys the following dynamical equations:

$$RC_1\dot{X} = -\frac{R}{R_1}Y,$$

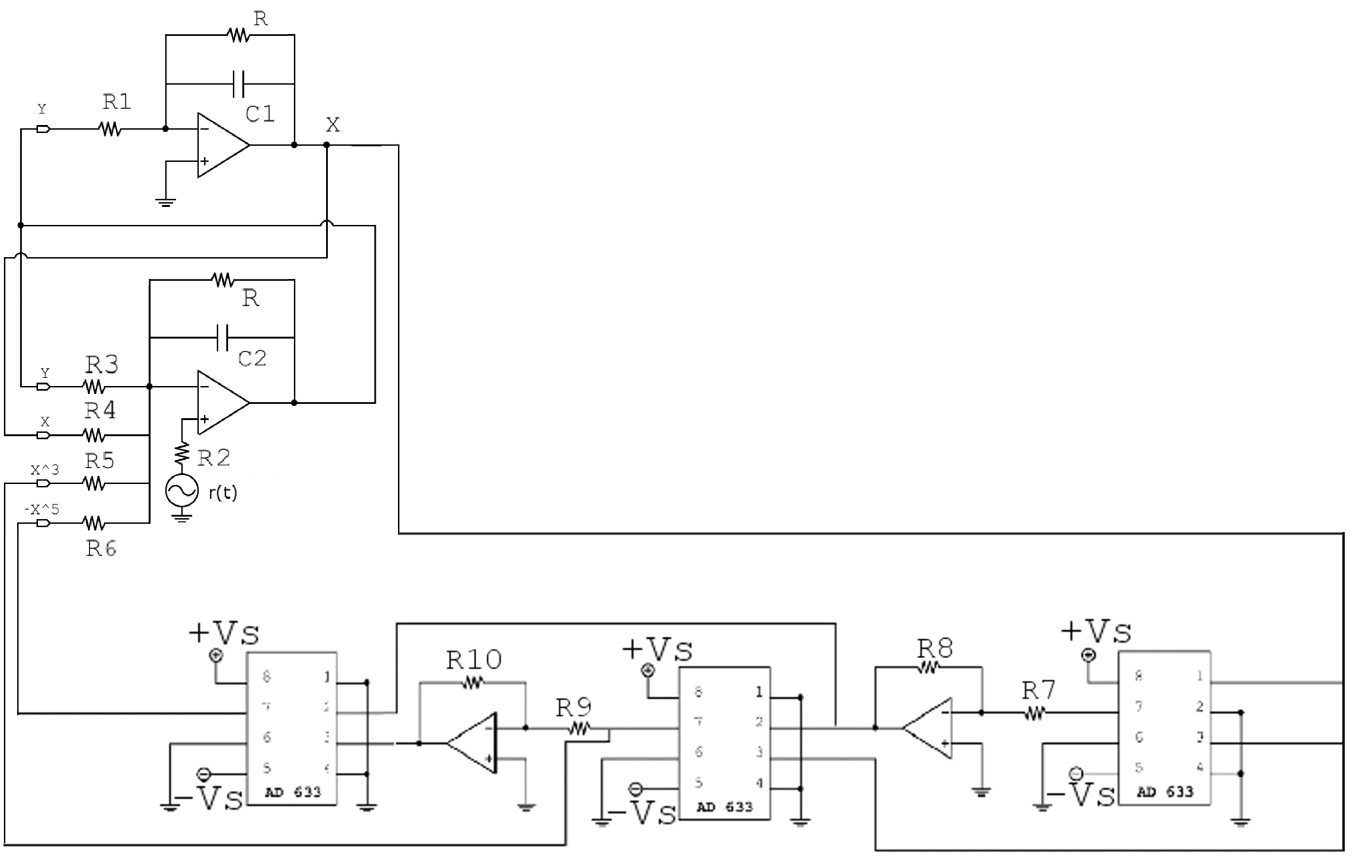

Fig. 17. Implementation of Circuits 2 and 3: Schematic of the single block implementing $G_i(s)$ and the related nonlinearity. Circuit component values: for $G(s)$, $R = R_1 = R_2 = R_4 = 1\,\text{k}\Omega$, $R_3 = 50\,\text{k}\Omega$, $R_5 = 100\,\text{k}\Omega$, $C_1 = C_2 = 8.2\,\mu\text{F}$, $Vs = \pm 18\,\text{V}$, $R_5 = 1.98\,\text{k}\Omega$, $R_6 = 6.25\,\text{k}\Omega$, $R_7 = R_9 = 10\,\text{k}\Omega$, $R_8 = R_{10} = 100\,\text{k}\Omega$, $TL084$ OP-AMPs and $AD633$ analog multipliers have been used.

$$RC_2\dot{Y} = -\frac{R}{R_4}Y - \frac{R}{R_5}X - \frac{R}{R_5}(-X^3) - \frac{R}{R_6}(-X^5) + \frac{R}{R_2}r(t), \tag{A.2}$$

where resistor values are chosen in order to match Eqs. (A.2) and Eqs. (A.1) with the desired parameter values. The effect of choosing the capacitors C_1 and C_2 is to introduce a temporal scaling factor to the equations as

$$\tau = \kappa t$$

where $\kappa = \frac{1}{RC_1} = \frac{1}{RC_2}$, with $R = 1\,\mathrm{k}\Omega$. The quintic nonlinearity is implemented by using three cascading analog multipliers. Furthermore, voltage at Y is taken as the output of each block.